

# Cross-field diffusion in low-temperature plasma discharges of finite length\*

Davide Curreli<sup>1</sup> and Francis F Chen<sup>2</sup>

<sup>1</sup> Nuclear, Plasma and Radiological Engineering, University of Illinois at Urbana Champaign, Urbana, IL 61801, USA

<sup>2</sup> Electrical Engineering Department, University of California, Los Angeles, 90095-1594, USA

E-mail: [dcurreli@illinois.edu](mailto:dcurreli@illinois.edu) and [ffchen@ee.ucla.edu](mailto:ffchen@ee.ucla.edu)

Received 17 September 2013, revised 26 August 2014

Accepted for publication 15 September 2014

Published 27 October 2014

## Abstract

The long-standing problem of plasma diffusion across a magnetic field ( $B$ -field) is reviewed, with emphasis on low-temperature linear devices of finite length with the magnetic field aligned along an axis of symmetry. In these partially ionized plasmas, cross-field transport is dominated by ion–neutral collisions and can be treated simply with fluid equations. Nonetheless, electron confinement is complicated by sheath effects at the endplates, and these must be accounted for to get agreement with experiment.

Keywords: cross-field diffusion, short-circuit effect, anomalous diffusion, low-temperature plasmas

(Some figures may appear in colour only in the online journal)

## 1. Classical diffusion

After almost a century of developments in plasma research, the diffusion of plasma across a magnetic field still remains a fundamental problem of interest in many applications. In the low-temperature plasmas typically used in the industry, like magnetrons or helicons, cross-field diffusion determines the transport phenomena and the properties of the discharge. In the high-temperature magnetically confined plasmas used for thermonuclear fusion, the cross-field diffusion regulates the fluxes from the hot core to the colder scrape-off layer at the edge, and consequently the fluxes to the plasma facing components, critical for the design of the machine. Interestingly, the same problem is of concern in both low-temperature and high-temperature plasmas, but for different reasons. Being of such wide interest, the topic has attracted considerable attention throughout the history of plasma physics. The literature available is so extensive that this review will be necessarily limited in scope. It is the aim of the present paper to review the major advancements in both theory and experiment, focusing attention on cross-field diffusion in partially ionized plasmas of finite length.

\* This article is part of the special issue ‘Transport in  $B$ -fields in low-temperature plasmas’, published in *Plasma Sources Sci. Technol.* vol 23, issue 4 (<http://iopscience.iop.org/0963-0252/23/4>).

In fully ionized plasmas, ‘classical’ diffusion arises from electron–ion Coulomb collisions with an arbitrary cut-off. In this case, diffusion is so slow that other effects, such as ‘Bohm diffusion’, arise from instabilities. Theories rarely agree with measured loss rates until nonlinear saturation of instabilities and the final turbulent state are accounted for. In fusion research, diffusion in toroidal devices is further complicated by the magnetic geometry, which spawns banana orbits and magnetic islands. Progress in understanding cross-field diffusion was made possible by the construction of linear machines with uniform  $B$ -fields. Such devices include, for instance, weakly ionized plasmas such as helicon discharges, and fully ionized Q-machines, with low electron temperatures  $KT_e$  of about 3 eV and 0.21 eV, respectively. The price one pays for such simple  $B$ -fields is that there are sheaths on the endplates, and these have to be treated properly, as is done in the paper.

## 2. Fluid theories on partially ionized plasmas

Cross-field diffusion in cold-plasma theory follows the equation of motion of ions in steady state [1–3]:

$$Mn(\mathbf{v} \cdot \nabla)\mathbf{v} = Zen(\mathbf{E} + \mathbf{v} \times \mathbf{B}) - \nabla p_i - Mn\nu\mathbf{v}, \quad (1)$$

where  $M$  is the ion mass,  $v$  the ion fluid velocity,  $n$  the plasma density,  $p_i$  the ion pressure  $nKT_i$ , and  $\nu$  the ions' collision frequency, which is dominated by charge-exchange collisions with neutrals; the other symbols are obvious. For simplicity, we have omitted the off-diagonal elements of the stress tensor, which contain the viscosity. A similar equation describes the electron fluid, but we shall find that electrons rarely follow that equation; rather, they tend to fall into a Maxwellian distribution and obey the Boltzmann relation. The anomalous mechanism of electron scattering and the surprising Maxwellization of the electron distribution in bounded domains have been observed even at very low collisionalities [4] and interpreted as plasma-boundary oscillations [5], non-local effects of electron kinetics [6], or convective ion-acoustic instabilities [7] near the discharge boundary. The nonlinear convection term  $v \cdot \nabla v$  will play an important role later but can be neglected for now. In the direction of  $B$ , or if  $B = 0$ , we can define the usual diffusion and mobility coefficients by solving for  $v$  with  $Z = 1$ :

$$v = \frac{1}{Mnv} (enE - KT\nabla n) = \frac{e}{Mv} E - \frac{KT}{Mv} \frac{\nabla n}{n}. \quad (2)$$

The coefficient of  $E$  is the ion mobility  $\mu_i$ , and the coefficient of  $\nabla n/n$  is the ion diffusion coefficient  $D_i$ . Similar definitions obtain for electrons, with  $\mu_e$  positive.

$$\begin{aligned} D_i &\equiv KT_i/Mv_i, & \mu_i &\equiv e/Mv_i \\ D_e &\equiv KT_e/Mv_e, & \mu_e &\equiv e/Mv_e. \end{aligned} \quad (3)$$

Ambipolar diffusion occurs when both species have the same flux  $nv_{i,e}$ :

$$\mu_i n E - D_i \nabla n = -\mu_e n E - D_e \nabla n. \quad (4)$$

In order for this to happen, there must be an electric field  $E$  given by

$$E = \frac{D_i - D_e}{\mu_i + \mu_e} \frac{\nabla n}{n}. \quad (5)$$

When this  $E$ -field is inserted into equation (4), the common ambipolar diffusion coefficient  $D_a$  is found to be

$$D_a = \frac{\mu_i D_e + \mu_e D_i}{\mu_i + \mu_e}. \quad (6)$$

This result applies only to diffusion *along*  $B$ , or when  $B = 0$ . For diffusion *across*  $B$ , we must use the perpendicular components of equation (1). Again with the nonlinear term neglected, these are, for either species,

$$\begin{aligned} v_x &= \pm \frac{eE_x}{mv} - \frac{KT}{mv} \frac{1}{n} \frac{\partial n}{\partial x} \pm \frac{eB}{mv} v_y = \pm \mu E_x - \frac{D}{n} \frac{\partial n}{\partial x} \pm \frac{\omega_c}{v} v_y \\ v_y &= \pm \frac{eE_y}{mv} - \frac{KT}{mv} \frac{1}{n} \frac{\partial n}{\partial y} \mp \frac{eB}{mv} v_x = \pm \mu E_y - \frac{D}{n} \frac{\partial n}{\partial y} \mp \frac{\omega_c}{v} v_x, \end{aligned} \quad (7)$$

where  $\pm$  stands for the sign of the charge, and where we have introduced the cyclotron frequency  $\omega_c \equiv eB/m$ , defined as positive for either species. It is customary now to replace  $\nu$  with its reciprocal  $1/\tau$  to obtain the familiar factor  $\omega_c \tau$ , whose

size reveals whether collisions destroy the cyclotron orbits or not. Simultaneous solution of equations (7) for  $v_x$  and  $v_y$  yields

$$\begin{aligned} v_y(1 + \omega_c^2 \tau^2) &= \pm \mu E_y - \frac{D}{n} \frac{\partial n}{\partial y} - \omega_c^2 \tau^2 \frac{E_x}{B} \pm \omega_c^2 \tau^2 \frac{KT}{eB} \frac{1}{n} \frac{\partial n}{\partial x} \\ v_x(1 + \omega_c^2 \tau^2) &= \pm \mu E_x - \frac{D}{n} \frac{\partial n}{\partial x} - \omega_c^2 \tau^2 \frac{E_y}{B} \mp \omega_c^2 \tau^2 \frac{KT}{eB} \frac{1}{n} \frac{\partial n}{\partial y}. \end{aligned} \quad (8)$$

The first two terms of each equation show that the mobility and diffusion coefficients for transport perpendicular to  $B$  are reduced by the magnetic field:

$$\mu_{\perp} = \frac{\mu}{1 + \omega_c^2 \tau^2}, \quad D_{\perp} = \frac{D}{1 + \omega_c^2 \tau^2}. \quad (9)$$

Electrons normally have large  $\omega_c$ 's and diffuse slowly across  $B$ . The last two terms of each equation (8) are the  $E \times B$  and diamagnetic drifts,  $v_E$  and  $v_D$ , reduced by a collisional factor.

$$v_E = \frac{E \times B}{B^2}, \quad v_D = \pm \frac{B \times \nabla p}{enB^2}. \quad (10)$$

Thus, the cross-field velocity for either species can be written succinctly as

$$v_{\perp} = \pm \mu_{\perp} E - D_{\perp} \frac{\nabla n}{n} + \frac{v_E + v_D}{1 + (v^2/\omega_c^2)}. \quad (11)$$

Many classic papers have been written on variations and applications of these results. For instance, there are books by Delcroix [8], Rozhansky and Tsedin [9], Shkarofsky *et al* [10], and others. Robson *et al* [11] have discussed collision cross sections. Fruchtmann [12] has extended such fluid theories to ambipolar and non-ambipolar diffusion in both linear and nonlinear regimes. Most theories assume infinite, one-dimensional half-spaces or infinite cylinders, neither of which exists in reality. In a long cylinder uniformly ionized at the edge by, say, radiofrequency (RF) antennas, one would expect that, in a strong  $B$ -field, the plasma density would be peaked at the edge because the electrons diffuse so slowly. However, this is rarely observed because finite plasmas have boundaries, and collisionless sheaths are needed there to equalize ion and electron losses and maintain quasineutrality of the plasma.

Particularly important are the sheaths on the surfaces ('endplates') which intersect the field lines of the  $B$ -field. Electrons can escape along  $B$  in nanoseconds unless they are repelled by the Coulomb barrier of a sheath. Ions enter the sheath at the Bohm speed [13], which is equal to the acoustic velocity  $c_s = (KT_e/M)^{1/2}$ , where  $M$  is the ion mass. Electrons enter with their one-dimensional thermal velocity  $v_{th} = (2KT_e/\pi m)^{1/2}$  and are repelled by a factor  $e^{V/KT_e}$ , where  $V$  is the (negative) sheath drop. Equating electron and ion fluxes to the endplates yields a sheath drop of  $-T_{eV}[1/2\ln(M/2\pi m)] \approx -4.7T_{eV}$  in argon (with  $T_i \ll T_e$ ), where  $T_{eV} = KT_e$  in electron-volts. Thus, if  $KT_e$  is about 3 eV in a gas discharge, there is a sheath drop of about 15 eV at the endplates. A similar calculation could be made for losses to the side boundary of a cylinder, but it would be inaccurate because electrons can oscillate at immeasurably

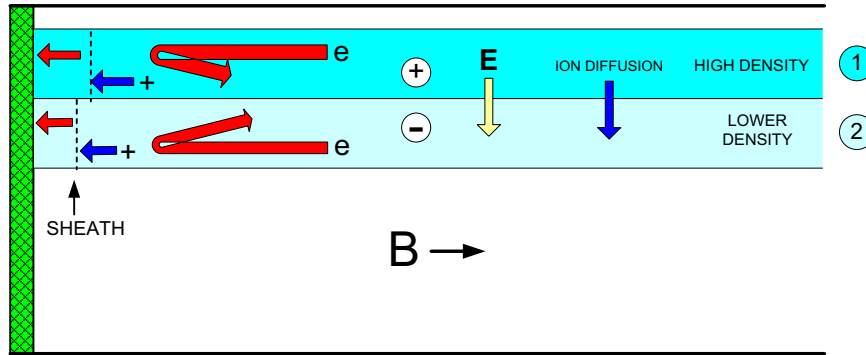


Figure 1. Initial sheath conditions at an endplate.

high frequency, and the cylinder may not be exactly aligned along  $B$ . At the endplates, however, an interesting mechanism called the Simon [14] ‘short-circuit’ effect occurs.

To illustrate this effect, consider a cylinder of radius  $a$  and length  $2L$  such that the ion flux at  $KT_i$  to the endplates is slow and can be neglected. Let the ionization source be localized at the radial edge. We wish to show that the density peak is nonetheless located on axis. Figure 1 shows one end of the discharge and the sheath conditions there. Initially, density  $n$  is higher in magnetic tube 1 near the edge. The sheath there must be thicker to repel more electrons, and that generates an inward-pointing  $E$ -field which drives ions inward. By adjustments of the sheath drop, the electron density can follow the ion density without actually moving across  $B$ . This allows electrons to be Maxwellian and follow the Boltzmann relation everywhere, but at the local temperature. The short-circuit effect cannot equalize  $KT_e$  across  $B$ -lines. Ultimately, the plasma is quasineutral and peaks on axis, even though ionization is at the edge [15]. By the Boltzmann relation, the plasma potential must also peak on axis, corresponding to an outward-pointing  $E$ -field, which drives the loss of ions to the edge. Thus, ‘classical diffusion’ in infinite cylinders is not easy to achieve because of the sheath effects at endplates.

If one assumes that the electrons are Maxwellian everywhere, a consequence is that the plasma density profile  $n(r)$  has a ‘universal’ shape independent of the pressure  $p$  and discharge radius  $a$ . Equation (1) in its full form is [16]:

$$Mv\nabla \cdot (nv) + Mnv \cdot \nabla v - enE + Mn\nu_{io}v = en(v \times B) - KT_i \nabla n \approx 0. \quad (12)$$

The first term represents drag due to injection of slow ions by ionization,  $\nu_{io}$  is the frequency of ion–neutral charge-exchange collisions, and the terms on the right can be neglected. The ion temperature is small; and the  $(v \times B)$  term, which describes ion Larmor orbiting, is small if the ion Larmor radius at the electron temperature is much larger than  $a$ .  $T_e$  is used here because ions are accelerated by electric fields scaled to  $T_e$ . Defining the ionization and collision probabilities as

$$P_i(r) \equiv \langle \sigma v \rangle_{\text{ion}}(r), \quad P_c(r) \equiv \langle \sigma v \rangle_{\text{cx}}(r) = \nu_{io}/n_n, \quad (13)$$

where  $n_n$  is the density of neutrals, we can combine equation (12) with the equation of continuity

$$\nabla \cdot (nv) = nn_n P_i(r) \quad (14)$$

to obtain

$$Mv \cdot \nabla v - eE + Mn_n(P_i + P_c)v = 0. \quad (15)$$

Ions will move slowly along  $B\hat{z}$  because electron conductivity prevents any large  $E_z$  from arising. Thus, we need consider only the  $r$  component of equation (15). With the usual definitions

$$E = -\nabla\phi, \quad \eta \equiv -e\phi/KT_e, \quad c_s \equiv (KT/M)^{1/2}, \quad (16)$$

the radial components of equations (15) and (14) become

$$v \frac{dv}{dr} = c_s^2 \frac{d\eta}{dr} - n_n(P_c + P_i)v \quad (17)$$

$$\frac{dv}{dr} + v \frac{d(\ln n)}{dr} + \frac{v}{r} = n_n P_i(r), \quad (18)$$

where we have dropped the subscript from  $v_r$ . The local electron Boltzmann relation, given by

$$n = n_0 e^{e\phi/KT_e} = n_0 e^{-\eta}, \quad \frac{d(\ln n)}{dr} = -\frac{d\eta}{dr}, \quad (19)$$

can be inserted into equation (18) to obtain

$$\frac{dv}{dr} + v \frac{dn}{dr} + \frac{v}{r} = n_n P_i(r). \quad (20)$$

Finally,  $d\eta/dr$  can be inserted from equation (17) to obtain, after a few steps,

$$\frac{dv}{dr} = \frac{c_s^2}{c_s^2 - v^2} \left[ -\frac{v}{r} + n_n P_i(r) + \frac{v^2}{c_s^2} n_n (P_i + P_c) \right]. \quad (21)$$

Note that  $dv/dr$  becomes infinite when  $v$  approaches  $c_s$ , leading to a natural transition to the thin, collisionless Debye sheath. The nature of equation (21) becomes clear if we introduce the dimensionless quantities

$$u \equiv v/c_s, \quad \rho \equiv (n_n P_i/c_s)r, \quad \text{and} \quad k(r) \equiv 1 + P_c(r)/P_i(r), \quad (22)$$

obtaining

$$\frac{du}{d\rho} = \frac{1}{1 - u^2} \left[ 1 + ku^2 - \frac{u}{\rho} \right]. \quad (23)$$

Solution of this equation will yield the radial profiles of  $n$ ,  $v$ , and  $\phi$ . The properties of the plasma are contained in  $k(r)$ ,

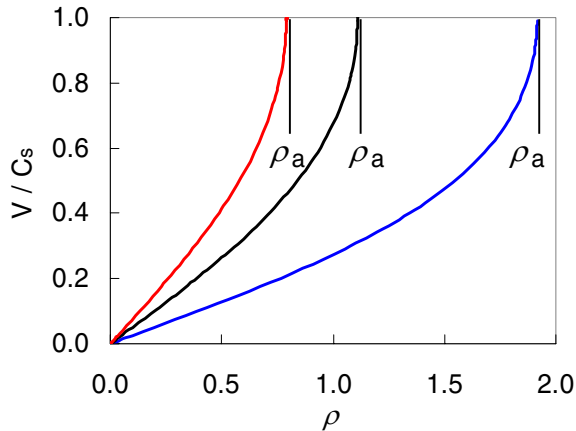


**Figure 2.** Solution of equation (23) for three values of  $k$ .

and these properties are only the ratio  $P_c/P_i$ . Equation (23) has been solved in equation (16) together with equations for neutral depletion and input-output balance in each radial shell. Here we show results for uniform  $T_e$  and  $n_n$ . Figure 2 shows  $u(\rho)$  for three values of  $k$ . The slope becomes infinite at different values  $\rho_a$ , which should be identified with the sheath edge at  $r = a$ . Rescaling  $\rho$  to the same  $r/a$ , one obtains the plot of  $u$  versus  $r/a$  in figure 3, together with corresponding profiles of  $n/n_0$  and  $\eta$ . Since  $P_c$  and  $P_i$ , and hence  $k$ , are independent of  $n_n$ , these profiles are independent of pressure and of the numerical value of  $a$ . They are ‘universal’ in that sense, but they will vary if  $KT_e$  changes.

The result is that classical diffusion in discharges of reasonable length is quite different from that in an infinite cylinder. The density, and hence potential, has to be peaked on axis in order to drive the ions out radially. They cannot be driven toward the axis in steady-state equilibrium because there is no fast way to escape from there.

Experimentally, the unexpected central peaking of density in edge-ionized plasmas was reported by Evans and Chen [17]. This was explained by the time-averaged Lorentz force on the electrons in the RF field, which caused the electron trajectories to cross through the central region, building up their density there and attracting the ions with the resulting  $E$ -field. That mechanism was for an infinite cylinder and would be changed by the presence of endplates.

### 3. The heritage of anomalous diffusion

In most experimental plasma devices, cross-field diffusion is observed to be non-classical, and the previous fluid theories are applicable only in first approximation. There is currently no general consensus on which theory to use to describe electron cross-field transport. In low-temperature devices, anomalous electron diffusion has been observed in a broad variety of plasmas with a wide range of ionization fractions. In high-temperature devices the additional complication of ion transport has been much better addressed by dedicated theoretical and experimental efforts. Nowadays the anomalous corrections to the ion neoclassical transport have a much better theoretical framework than the electron transport.

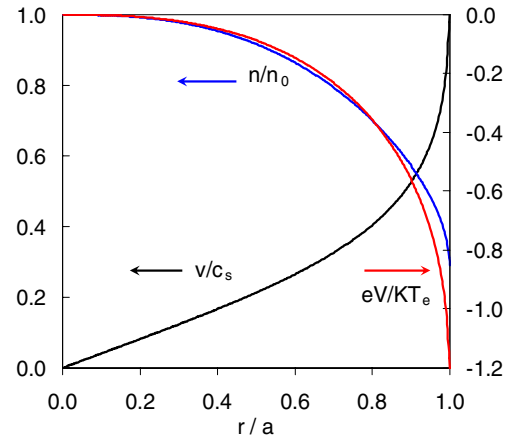


**Figure 3.** Renormalized profiles of  $n$ ,  $v$ , and  $\phi$ .

Since electron anomalous diffusion was initially observed in elongated low-temperature partially ionized plasma tubes, we will now review the historical development and comment. Hoh and Lehnert [45] did a famous series of measurements using electropositive gases, confirmed also by Allen *et al* [46], showing that the agreement between experiment and classical diffusion theory was valid only up to a certain critical magnetic field. At magnetic fields higher than the critical value, a much higher diffusion was present. Above the critical magnetic field, the discharge loses its axial symmetry, and exhibits regular oscillations appearing as rotating helical structures [47]. In Hoy and Lehnert’s experiment they used tubes long enough (tube length greater than 50 times tube diameter) that any short-circuit effect as described by Simon [14] was suppressed. Hoh advanced the idea that above the critical magnetic field, a wall sheath instability might occur. Kadomtsev and Nedospasov [47] explained the phenomenon from a different standpoint. They studied harmonic perturbations of the form  $\exp(im\phi + ikz - i\omega t)$  in a diffusion model including fluid magnetized electrons. Their dispersion relation led to the calculation of the correct analytical value of the critical magnetic field, the correct description of the onset of anomalous diffusion, and the calculation of the frequency of oscillation of the unstable mode. Their model was in successful agreement with the measurements done by Hoh and Lehnert. The limitations of using a hydromagnetic fluid model in low-density collisionless plasmas were described later by Schmidt [48], who used a ‘self-consistent’ guiding-center model to describe the plasma motion across the magnetic field. His approach gave more detailed information on plasma behavior (e.g. the discussion of a polarization layer), but no comparison with experiments was given.

Despite the success of the Hoh–Lehnert experiments and of the Kadomtsev–Nedospasov theory, the measurements were still controversial. Other authors [49, 50] reported diffusion in agreement with classical rates ( $D \sim 1/B^2$ ) in shorter cylindrical discharges at high levels of ionization even in strong magnetic fields. Classical rates were calculated also for fully ionized plasmas. Maintaining a fully ionized plasma in equilibrium normally requires a fusion confinement

device in the form of a torus or magnetic mirror. In these machines, unavoidable instabilities enhance diffusion well above the classical rate based on ion–electron collisions. The diffusion rates, originally calculated by Spitzer [18], have been summarized by Book and published by Huba [19]. In thermal plasmas with temperatures  $T_i$  and  $T_e$  and no beams, the classical diffusion coefficient for drifts across  $B$  is given by

$$D_{\perp} \approx 10^{-4} Z n \ln \Lambda (K T_e + K T_i) / B^2 \Omega \text{ m}, \quad (24)$$

where  $\ln \Lambda$  is the Coulomb logarithm, a weakly varying number of the order of 10. Note that  $D_{\perp}$  decreases as  $1/B^2$ , in contrast with Bohm diffusion, which goes at the rate

$$D_B = \frac{1}{16} \frac{K T_e}{e B}, \quad (25)$$

which decreases more slowly with  $B$  and could be several orders of magnitude larger. In early experiments plasma losses occurred at a faster Bohm rate than the classical rate. Spitzer once tracked down David Bohm in Brazil and asked him how the factor  $1/16$  was derived. Bohm did not remember! The  $1/B$  ‘Bohm diffusion’ was interpreted by Bryan Taylor [51] as the maximum value which the transverse diffusion can ever attain. At that time Taylor was investigating the correlation function of the fluctuating electric field in a plasma [52] as a means for the calculation of the mean force on a slowly moving test charge, and ultimately obtain the transport coefficients. Taylor applied his method to the problem of diffusion of ions across a magnetic field [53]. He found that ion diffusion was driven by three contributions, two of which arose from the mean force on the ion, and the third one from the fluctuations. For the case of different ion and electron temperatures,  $T_i \neq T_e$ , Taylor’s method suggested results substantially different than that of the classical Chapman–Enskog expansion.

Guest and Simon [54] extended the Kadomtsev–Nedospasov model to the cases of  $B$ -fields higher than a critical threshold or of background pressures below a critical value. According to their interpretation, in a magnetized plasma column at low pressure the different azimuthal streams of ions and electrons are the main driving force of the instability. The difference in the streams generates an oscillating electric field  $E_{\theta}$  in the azimuthal direction that in turn increases radial diffusion via the  $E_{\theta} \times B$  drift. The frequency of the oscillating azimuthal  $E_{\theta}$  field was approximately equal to  $\omega_{\text{rot}} \approx \pi / (4L) m_i (1 + T_e / T_i)$ , where  $L$  is the discharge length and  $\mu_i$  is the average ion velocity to the end walls. Despite the evident role of the plasma angular momentum, no explicit calculation of this quantity was done. Further experiments using cesium plasmas and comparison with calculations supported the transition from classical to anomalous diffusion, also confirming Bohm diffusion as the maximum limiting value of the process.

Chen [55, 56] found that even the reflex arc works only because of cross-field diffusion caused by the  $E \times B$  instability. In the reflex arc, the arc is in a dc magnetic field and the cathodes (either cold or thermionic) are at each end. The anode surrounds the plasma; as a consequence, the discharge current can flow only across the  $B$ -field. A further important step in

understanding the instabilities in crossed electric and magnetic fields was made by Simon [57] (Simon–Hoh instability). Simon showed that when a strong electric field is applied across the magnetic field in a non-uniform plasma, the discharge becomes unstable. The instability occurs when the electric field is *in the same direction* as the density gradient. In the reflex arc this is the direction of the applied ionizing potential, and only the instability allows the discharge current to flow. A different, original approach to the problem of cross-field diffusion was proposed by Kurşunoğlu [58], who used stochastic theory to sample the Langevin equation and follow the Brownian motion of charged particles across the field lines. He derived expressions of both classical and ‘enhanced’ diffusion coefficients.

The subject of anomalous diffusion became so important that an Anomalous Absorption Conference series was started and has persisted for over four decades. At the end of the last century Bohm’s anomalous transport was predominantly interpreted as an upper limiting value of cross-field diffusion [59], with low-frequency drift-wave fluctuations playing the major role in enhancing classical diffusion [60]. At small amplitudes of the fluctuating azimuthal  $E$ -field the diffusion remains classical; when the amplitude of the oscillation is increased, the diffusion gradually shifts to the anomalous  $1/B$  trend [61]. In fusion devices, electron drift instabilities can be suppressed by such mechanisms as shear, minimum- $B$ , and short connection length. Similar instabilities can be driven by other energy sources, such as ion temperature gradients.

Any plasma with a density gradient, which includes any confined plasma, suffers from a universal instability discovered by Sagdeev and Chen [41] called a resistive drift wave instability. A Langmuir probe inserted into a Q-machine would show a turbulent spectrum of electrostatic oscillations which caused anomalously rapid diffusion across  $B$ . By applying a voltage on an aperture limiter, the instability could be brought near threshold so that it could be seen as a sine wave oscillation [42]. In a cylinder, a drift wave propagates azimuthally in the electron diamagnetic drift direction and has a long wavelength in the direction of  $B$ . Its azimuthal electric field causes an oscillating radial drift of both ions and electrons. When the wave is growing, the radial drift is out of phase with the density perturbation, such that the drift is outward when the density is high and inward when the density is low. Thus, there is a net transport of plasma toward the boundary. In the nonlinear state, the plasma can be envisioned as escaping in ‘blobs’ [43], and these have been observed in fusion devices [44].

The mechanism of resistive drift waves is illustrated in figure 4, showing the edge region in one cross section of the plasma. The density profile of an azimuthal perturbation, a component of noise, is shown in the shaded plasma region. When the Boltzmann relation is satisfied, the potential  $\phi_1$  is in sync with the density perturbation, as shown by the + and – signs in column 1. The resulting electric field  $E_1$  causes an  $E_1 \times B_0$  drift which is  $90^\circ$  out of phase with  $n_1$  and is seemingly harmless. These drifts bring denser plasma in from the plasma interior. However, the  $E_1 \times B_0$  drifts are not equal for ions and electrons because the finite-Larmor-radius effect slows down the ions more than the electrons. Consider the

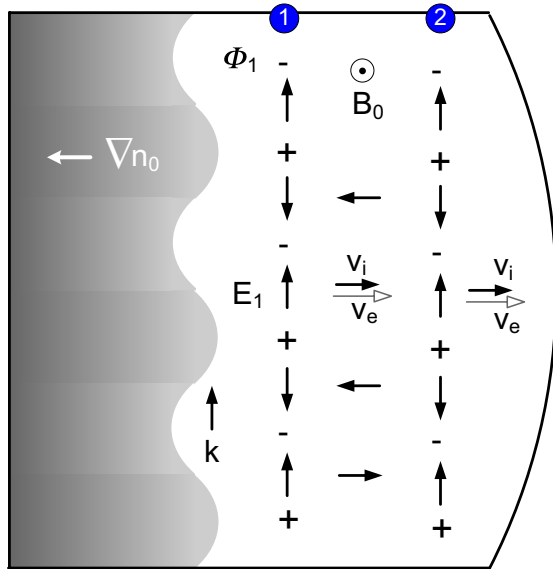


Figure 4. The mechanism of resistive drift waves.

situation at the center of the diagram. Electrons are drifting in faster, so a negative charge accumulates, shifting the  $\phi_1$  distribution downward, as in column 2. Now the  $E_1 \times B_0$  drifts are shifted so that more plasma is brought in where the density is already higher than normal, and vice versa, so the perturbation grows.

To be unstable, such a perturbation must have long wavelength along  $B_0$  so that electrons cannot short circuit the  $E$ -field by moving along  $B_0$ . There must be finite resistivity; hence the name resistive drift. The  $n$ - $\phi$  phase shift can be measured even if the unstable wave has reached a constant amplitude due to damping or nonlinear saturation. It is an important characteristic of instabilities and is often measured with correlation techniques [20].

Though classical diffusion in fully ionized plasmas has not been achieved in fusion research, it has been observed in two experimental inventions: Q-machines [21] and machines with levitated internal conductors, such as octopoles [22, 23]. Multipole machines, which have internal ring conductors either levitated magnetically or supported by thin wires, can produce minimum- $B$  volumes where  $|B|$  increases in all directions. Plasmas created there are stable and can diffuse classically. Q-machines produce plasma by thermal injection. Electrons are emitted from tungsten ‘cathodes’ heated to 2400 K at the ends of uniform  $B$ -field lines. Atoms of sodium or potassium are injected toward the cathodes, where they are ionized upon contact, since their ionization potentials are smaller than the work function of the tungsten. Thus, a thermal plasma at 2400 K is formed without any applied electric fields. Nonetheless, spontaneous oscillations were observed [24] which caused enhanced diffusion [25], as explained below. By applying magnetic shear with a current through a 1 cm diameter aluminum tube strung through holes in the hot cathodes, Chen and Mosher [26] quenched the oscillations and brought the diffusion down to within a factor 2 of classical.

#### 4. Cross-field electron kinetics

Fluid models of cross-field transport, as those described in section 2, are convenient for rapid but approximate descriptions of the macroscopic behavior. In low-temperature conditions, ions are well described by fluid models, since their kinetic behavior is negligible. However, electrons exhibit features that cannot entirely be taken into account within the fluid framework, and a kinetic treatment is sometimes required. There are cases where the electron distribution function can be driven far from a Maxwellian state.

A complete theoretical treatment of the electron cross-field kinetics has never been fully developed, even if statistical mechanics offers the proper framework for such analysis. The full kinetic behavior of  $N$  free classical particles (both charged and neutrals) immersed in a magnetic field is formally described by Liouville’s theorem of the time evolution of the phase-space distribution function. The Liouville theorem can opportunely be rewritten (Bogolyubov [27], Born and Green [28], Kirkwood [29, 30], Yvon [31] (BBGKY)) as a hierarchy of integro-differential equations relating the  $k$ -particle distribution function  $f_k$  to the  $k + 1$  particle distribution function  $f_{k+1}$ . Even if the BBGKY hierarchy does not have any more information than Liouville’s theorem, it is much more useful. It allows the chain to be cut off at some stage, and to make clear the error which occurs in the cut-off. Typical truncations of the hierarchy are at the order zero, giving the Vlasov equation,

$$\frac{\partial f_0}{\partial t} + \mathbf{v} \cdot \nabla_r f_0 + \mathbf{a} \cdot \nabla_v f_0 = 0 \quad (26)$$

or at the first order, giving the Boltzmann equation:

$$\frac{\partial f_1}{\partial t} + \mathbf{v} \cdot \nabla_r f_1 + \mathbf{a} \cdot \nabla_v f_1 = C_1(f_2). \quad (27)$$

In the Boltzmann model, only two-body interactions (electron–electron, electron–neutral, electron–ion, and so on) are included for the evaluation of the collision integral  $C_1(f_2)$ . The termination of the chain at such low order is, however, critical, since it introduces an error. When the distribution function is not too far from a state of statistical equilibrium (Maxwellian distribution), the error committed in the truncation of the chain is of order  $g^k$ , where  $k$  is the order of truncation, and  $g \propto (n/T_e^3)^{1/2}$  is the inverse of the classical plasma parameter. The parameter  $g$  is proportional to the ratio of the average interaction energy between particles to their average kinetic energy. When  $g$  is increased, the distribution function departs from a Maxwellian, and kinetic effects become gradually more relevant. At high  $g$ ’s ( $g \gg 1$ ) the truncation of the hierarchy at the first order (Boltzmann equation) loses its validity, and higher orders of the hierarchy are necessarily required. Models of electron kinetics are typically truncated at the first order of the BBGKY, so that only a solution of the Boltzmann equation is sought.

The solution of the electron Boltzmann equation can be obtained using both analytical and numerical tools. The Chapman–Enskog method [32] and Grad’s moment method [33] are two powerful analytical methods to find approximate

solutions of the Boltzmann equation. The first is based on the expansion of the distribution function in terms of associated Laguerre polynomials [34]. The latter expands the distribution function in a series of tensorial Hermite polynomials. Both methods involve series expansions, which must be truncated at some order for practical calculations. The truncation of the series introduces an additional error into the description of the cross-field electron kinetics. Numerical methods for solution of the electron Boltzmann equation are typically based on one of the following techniques: (1) an implementation of the Chapman–Enskog or Grad’s solution, with the series truncated at some convenient order, (2) a discretization of the operators of equation (27) using finite differences, finite-volumes, and quadratures of the integral operator, or (3) a discretization of the solution using finite elements.

The solution of the Boltzmann equation gives a first insight into the cross-field electron kinetics. Druyvesteyn [35] first derived the electron velocity distribution function in a uniform electric field for the simple case of impacts with velocity-independent cross sections; cf Smirnov [36]. Druyvesteyn’s result can easily be generalized to the case of crossed electric and magnetic fields by solving the stationary and spatially uniform Boltzmann problem for the case  $\mathbf{E} = E_x \hat{x}$  and  $\mathbf{B}_0 = B_z \hat{z}$ . To simplify the calculation, we assume weakly ionized conditions. Then, the density of electrons is much lower than that of the neutral gas, and electron–neutral collisions are by far the most frequent collision event:  $\nu_{eo} \gg \nu_{ei}$ . The electron–electron collision frequency can be neglected since these only maintain the Maxwellian distribution. Expanding the distribution function into three terms (spherical contribution, electric field contribution, and  $\mathbf{E} \times \mathbf{B}$  drift),

$$f(v) = f_0(v) + v_x f_1(v) + v_y f_2(v) \quad (28)$$

and expressing the collision integral as

$$C(f) = C(f_0) - \nu_{eo} v_x f_1 - \nu_{eo} v_y f_2, \quad (29)$$

where the collision integral  $C(f_0)$  for elastic collisions of electrons with the background gas at temperature  $T_0$  is obtained by solving the Fokker–Planck equation, we have

$$C(f_0) = \frac{m}{M} \frac{KT_0}{v^2} \frac{\partial}{\partial v} \left[ v^3 \nu_{eo} \left( \frac{f_0}{KT_0} + \frac{1}{mv} \frac{\partial f_0}{\partial v} \right) \right]. \quad (30)$$

Substituting equations (28), (29), and (30) into the Boltzmann equation (30), the following solution is found for the electron velocity distribution function:

$$f_0(v) = a_0 \exp \left[ - \int_0^v \frac{mv}{KT_0 + e^2 M E_x^2 / (3m^2(v_{eo}^2 + \omega_{ce}^2))} dv \right] \quad (31)$$

$$f_1(v) = - \left( \frac{e E_x v_{eo}}{v_{eo}^2 + \omega_{ce}^2} \right) \frac{1}{mv} \frac{\partial f_0}{\partial v} \quad (32)$$

$$f_2(v) = - \frac{\omega_{ce}}{v_{eo}} f_1(v), \quad (33)$$

where the normalization constant  $a_0$  is a function of the density. When the magnetic field is zero ( $\omega_{ce} \rightarrow 0$ ), the solution (31)–(33) returns the classical Druyvesteyn distribution in the

absence of a magnetic field, with  $f_2(v) = 0$ . Integrating equations (31)–(33) over the spherically symmetric part  $f_0(v)$  of the distribution function, the drift velocity of electrons in direction perpendicular to the  $\mathbf{B}$ -field can be derived:

$$u_{e,x} = \frac{e E_x}{3m} \int \frac{1}{v^2} \frac{d}{dv} \left( \frac{v_{eo} v^3}{v_{eo}^2 + \omega_{ce}^2} \right) f_0(v) dv \quad (34)$$

$$u_{e,y} = - \frac{e E_x \omega_{ce}}{3m} \int \frac{1}{v^2} \frac{d}{dv} \left( \frac{v^3}{v_{eo}^2 + \omega_{ce}^2} \right) dv. \quad (35)$$

Equations (34) and (35) are an approximate solution of the electrons’ cross-field kinetics in weakly ionized conditions. The two components  $x$  and  $y$  are both in the direction perpendicular to the magnetic field, with  $x$  being along the electric field and  $y$  along the  $\mathbf{E} \times \mathbf{B}$  direction. The limiting case of equations (34) and (35) for strong magnetic fields  $\omega_{ce} \rightarrow \infty$  gives:

$$u_{e,x} \ll u_{e,y}, \quad u_{e,y} = -e E_x / m \omega_{ce}. \quad (36)$$

Equation (36) shows that at strong magnetizations the main drift motion is along the  $\mathbf{E} \times \mathbf{B}$  direction and is independent of the collision frequency. A similar procedure can be extended also to weakly ionized ions [37], adding dedicated treatments of ion–neutral collisions and of charge-exchange processes. The equal mass of ions and neutrals involves significant momentum transfer among the two species. Charge-exchange usually determines a significant deceleration of the ion fluid, causing the so-called charge-exchange drag. The concurrent effect of charge-exchange deceleration and ionization (new ions generated at rest) can be seen at a macroscopic fluid level from the parameter  $k(r)$  in equation (22). Kinetic calculations including finite-size effects [38, 39] show the possibility of controlling the discharge parameters by modifying the short-circuiting conditions at the plasma wall. An extensive review giving experimental evidence of the relevance of the short-circuiting conditions for electron kinetics is given by Zhilinskii and Tsendin [40].

## 5. Summary

In discharges in which the  $\mathbf{B}$ -field intersects endplates, the sheaths on the endplates will self-adjust to equalize ion and electron fluxes on each field line. The appearance that electrons have crossed the  $\mathbf{B}$ -field to follow the faster cross-field motion of the ions is called the Simon short-circuit effect. In very long discharges or those with closed magnetic surfaces, the azimuthal  $\mathbf{E} \times \mathbf{B}$  drifts of the electrons and ions are not equal because of finite Larmor radius effects. In the presence of the necessary pressure gradient in a confined plasma, a drift-wave instability can then arise with an azimuthal wavelength. The wave causes an oscillating radial drift of the plasma such that the drift is outward when the density is high and inward when the density is low, leading to enhanced plasma losses to the wall. This loss rate is proportional to the phase shift between the  $\tilde{n}$  and  $\tilde{\phi}$  oscillations of the drift wave.

## References

- [1] Chen F F 1984 *Introduction to Plasma Physics and Controlled Fusion* vol 1 *Plasma Physics* 2nd edn (New York: Plenum) p 157
- [2] Goldston R J and Rutherford P H 1995 *Introduction to Plasma Physics* (Bristol: Institute of Physics Publishing) p 85
- [3] Lieberman M A and Lichtenberg A J 2005 *Principles of Plasma Discharges and Materials Processing* 2nd edn (Hoboken, NJ: Wiley) chapter 5
- [4] Langmuir I 1925 Scattering of electrons in ionized gases *Phys. Rev.* **26** 585
- [5] Gabor D, Ash E A and Dracott D 1955 Langmuir's paradox *Nature* **176** 916
- [6] Tsengin L D 2003 Current trends in electron kinetics of gas discharges *Plasma Sources Sci. Technol.* **12** S51
- [7] Baalrud S D, Callen J D and Hegna C C 2009 Instability-enhanced collisional effects and Langmuir's paradox *Phys. Rev. Lett.* **102** 245005
- [8] Delcroix J-L 1960 *Introduction to the Theory of Ionized Gases* (New York: Interscience)
- [9] Rozhansky V A and Tsengin L D 2001 *Transport Phenomena in Partially Ionized Plasma* (Boca Raton, FL: Taylor and Francis)
- [10] Shkarofsky I P, Bachynsky T W and Watson M P 1967 *The Particle Kinetics of Plasmas* (Reading MA: Addison-Wesley)
- [11] Robson R E, White R D and Petrovic Z Lj 2005 Physically based fluid modeling of collisionally dominated low-temperature plasmas *Rev. Mod. Phys.* **77** 1303
- [12] Fruchtman A 2008 Ambipolar and nonambipolar cross-field diffusions *Plasma Sources Sci. Technol.* **18** 025033
- [13] Lieberman M A and Lichtenberg A J 2005 *Principles of Plasma Discharges and Materials Processing* 2nd edn (Hoboken, NJ: Wiley) p 169 chapter 5
- [14] Simon A 1955 *Phys. Rev.* **98** 317
- [15] Chen F F and Curreli D 2013 Central peaking of magnetized gas discharges *Phys. Plasmas* **20** 057102
- [16] Curreli D and Chen F F 2011 Equilibrium theory of cylindrical discharges with special application to helicons *Phys. Plasmas* **18** 113501
- [17] Evans J D and Chen F F 2001 Nonlocal power deposition in inductively coupled plasmas *Phys. Rev. Lett.* **86** 5502
- [18] Spitzer L 1962 *Physics of Fully Ionized Gases* 2nd edn (New York: Interscience)
- [19] Huba J D 2011 Plasma Formulary *Naval Research Laboratory Report NRL/PU/6790-94-265*
- [20] Tynan G R, Burin M J, Holland C, Antar G and Diamond P H 2004 *Plasma Phys. Control. Fusion* **46** A373
- [21] Chen F F and Mosher D 1967 Shear stabilization of a potassium plasma *Phys. Rev. Lett.* **18** 639
- [22] Tamano T, Prater R and Ohkawa T 1971 Diffusion of a plasma with a small dielectric constant in the dc octopole *Phys. Rev. Lett.* **27** 18
- [23] Kerst D W, Dory R A, Wilson W E, Meade D M and Erickson C W 1965 Motion of plasma and lifetimes of energetic ions in a toroidal octupole magnetic field *Phys. Rev. Lett.* **15** 396
- [24] D'Angelo N and von Goeler S 1965 Plasma losses in a Q-device *Nucl. Fusion* **5** 279
- [25] Hendel H W, Chu T K and Politzer P A 1968 Collisional drift waves—identification, stabilization, and enhanced plasma transport *Phys. Fluids* **11** 2426
- [26] Chen F F and Mosher D 1967 Shear stabilization of a potassium plasma *Phys. Rev. Lett.* **18** 639
- [27] Bogoliubov N N 1946 Kinetic equations *J. Phys. USSR* **10** 265
- [28] Born M and Green H S 1946 A general kinetic theory of liquids: I. The molecular distribution functions *Proc. R. Soc. A* **188** 10
- [29] Kirkwood J G 1946 The statistical mechanical theory of transport processes: I. General theory *J. Chem. Phys.* **14** 180
- [30] Kirkwood J G 1947 The statistical mechanical theory of transport processes: II. Transport in gases *J. Chem. Phys.* **15** 72
- [31] Yvon J 1935 La théorie statistique des fluides et l'équation d'état *Actual. Sci. Indust.* no. 203 (Paris: Hermann)
- [32] Chapman S and Cowling T G 1952 *The Mathematical Theory of Non-uniform Gases: An Account of the Kinetic Theory of Viscosity, Thermal Conduction and Diffusion in Gases* (Cambridge: Cambridge University Press)
- [33] Grad H 1958 Principles of the kinetic theory of gases *Handbuch der Physik* vol XII, ed S Flügge (Berlin: Springer) pp 205–94
- [34] Sonine N J 1880 Sur les fonctions cylindriques et le développement des fonctions continues en séries *Math. Ann.* **16** 1–80
- [35] Druyvesteyn M J and Penning F M 1940 The mechanism of electrical discharges in gases of low pressure *Rev. Mod. Phys.* **12** 87
- [36] Smirnov B M 2001 *Physics of Ionized Gases* (New York: Wiley-Interscience)
- [37] Breizman B and Arefiev A V 2002 Ion kinetics in a magnetized plasma source *Phys. Plasmas* **9** 1015
- [38] Rozhansky V A and Tsengin L D 1994 Two-dimensional nonuniformly heated magnetized plasma transport in a conducting vessel *Phys. Rev. E* **50** 3033
- [39] Kaganovich I D, Rozhansky V A, Tsengin L D D and Veselova I Yu 1996 Fast expansion of a plasma beam controlled by short-circuiting effects in a longitudinal magnetic field *Plasma Source Sci. Technol.* **5** 743
- [40] Zhilinskii A P and Tsengin L D 1980 Collisional diffusion of a partially ionized plasma in a magnetic field *Sov. Phys.—Usp.* **2** 331
- [41] Moiseev S S and Sagdeev R Z 1964 *Sov. Phys.—Tech. Phys.* **9** 196  
Chen F F 1965 Excitation of drift instabilities in thermionic plasmas *J. Nucl. Energy C* **7** 399
- [42] Rogers K C and Chen F F 1970 Direct measurement of drift-wave growth rates *Phys. Fluids* **13** 513
- [43] Chen F F 1967 The leakage problem in fusion reactors *Sci. Am.* **217** 76
- [44] Maqueda R J, Wurden G A, Zweben S, Roquemore L, Kugel H, Johnson D, Kaye S, Sabbagh S and Maingi R 2001 Edge turbulence measurements in NSTX by gas puff imaging *Rev. Sci. Instr.* **72** 931
- [45] Hoh F C and Lehnert B 1960 Diffusion processes in a plasma column in a longitudinal magnetic field *Phys. Fluids* **3** 600
- [46] Allen T K, Paulikas G A and Pyle R V 1960 Instability of a positive column in a magnetic field *Phys. Rev. Lett.* **5** 409  
Gerjuoy E and Stuart G W 1960 Ionization growth in a gas with a constant electric field *Phys. Fluids* **3** 1008
- [47] Kadomtsev B B and Nedospasov A V 1960 Instability of the positive column in a magnetic field and the 'anomalous' diffusion effect *J. Nucl. Energy C* **1** 230
- [48] Schmidt G 1960 Plasma motion across magnetic fields *Phys. Fluids* **6** 961
- [49] D'Angelo N and Rynn N 1961 Diffusion and recombination of a highly ionized cold plasma in a magnetic field *Phys. Fluids* **4** 1303–6
- [50] D'Angelo N and Rynn N 1961 Diffusion of a cold cesium plasma across a magnetic field *Phys. Fluids* **4** 275–6
- [51] Taylor J B 1961 Diffusion of plasma across a magnetic field *Phys. Rev. Lett.* **6** 262
- [52] Taylor J B 1960 Electric field correlation and plasma dynamics *Phys. Fluids* **3** 792



- [53] Taylor J B 1961 Diffusion of plasma ions across a magnetic field *Phys. Fluids* **4** 1142
- [54] Guest G and Simon A 1962 Instability in low-pressure plasma diffusion experiments *Phys. Fluids* **5** 503
- [55] Chen F F 1962 The radial electric field in a reflex discharge *Phys. Rev. Lett.* **8** 234
- [56] Chen F F and Cooper A W 1962 Electrostatic turbulence in a reflex discharge *Phys. Rev. Lett.* **9** 333
- [57] Simon A 1963 Instability of a partially ionized plasma in crossed electric and magnetic field *Phys. Fluids* **6** 382
- [58] Kurşunoğlu B 1963 Brownian motion in a magnetic field *Phys. Rev.* **132** 21
- [59] Horton W 1999 Drift waves and transport *Rev. Mod. Phys.* **71** 735
- [60] Nielsen A H, Pécseli H L and Rasmussen J J 1996 Turbulent transport in low- $\beta$  plasmas *Phys. Plasmas* **3** 1530
- [61] Pettini M, Vulpiani A, Misguich J H, De Leener M, Orban J and Balescu R 1988 Chaotic diffusion across a magnetic field in a model of electrostatic turbulent plasma *Phys. Rev. A* **38** 344